Time-resolved luminescence of nanocrystalline inorganic complex oxides

V Pankratov[1], D Millers[1], L Grigorjeva[1], W Lojkowski[2], A Kareiva[3]

[1]Institute of Solid State Physics University of Latvia, 8 Kengaraga, LV-1063, Riga, Latvia

[2]Institute of High Pressure Physics, Sokolowska 29, 01-142, Warsaw, Poland

[3]Department of General and Inorganic Chemistry Vilnius University, Naugarduko 24, LT-2006 Vilnius, Lithuania

E-mail: vpank@latnet.lv

Abstract. Two types of complex nanosized oxides – cerium doped $Y_3Al_5O_{12}$ (YAG) and $CaWO_4$ – have been studied by means of time-resolved luminescence spectroscopy. Comparative study of time-resolve luminescence characteristics of cerium doped YAG single crystal, nanopowders and nanoceramic as well as for $CaWO_4$ macro- and nanocrystals has been done. Two components in the decay kinetic of Ce^{3+} related emission in YAG nanocrystals were detected and it was suggested that a different energy transfer rate to volume and surface Ce^{3+} ions takes place. It is shown that the segregation of Ce^{3+} ions near nanoparticles surface and/or dislocation lines plays a crucial role in degradation of light yield of cerium related luminescence in YAG nanocrystals. Time-resolved properties of sol-gel synthesized $CaWO_4$ nanocrystals depends strongly on the synthesis rout. It was shown that shallow traps have a strong influence on the luminescence decay times of nanosized $CaWO_4$.

1. Introduction

Inorganic phosphors and scintillators play an important role in various applications in scientific and industrial applications and increasingly for medical and security purposes [1-4]. Currently mainly inorganic single crystals are utilized in the mass production of scintillators and detectors. Fortunately a rapid development of nanotechnology allows replacing single crystalline materials with nanocrystals in the near future. However, a fabrication of transparent nanocrystalline ceramic is a significant problem which considerably restricts wide practical applications.

Cerium doped yttrium aluminum garnet ($Y_3Al_5O_{12}$ or YAG) and calcium tungstates ($CaWO_4$) are well-known efficient materials for transformation of invisible radiation into visible light [5-8]. Therefore these materials could be good candidates to be raw starting materials for transparent nanocrystalline ceramic. Recently it was reported that translucent nanosized ceramic of cerium doped YAG was already sintered [9-10]. However luminescent properties (especially time-resolved characteristics) of nanocrystalline cerium doped YAG is poorly studied so far. In [11] it was shown that some luminescence characteristics of cerium doped YAG nanopowders differ from those obtained for a single crystal. However a deeper understanding of energy transfer processes as well as properties

of luminescence center in nanocrystals is absolutely necessary. Therefore in present study a comparative analysis of time-resolved luminescence characteristics for cerium doped YAG single crystal, nanopowders and nanoceramics was carried out.

In contrast to cerium doped YAG, $CaWO_4$ is self-activated phosphor. It means that each regular $(WO_4)^{2-}$ anion complex can be a luminescence centre. Therefore luminescence properties of nanocrystalline $CaWO_4$ do not depend on the distribution of impurity ions in nanoparticle as well as on their segregation on the grain borders in ceramics. To date the reports of preparation on nanosized $CaWO_4$ are very rare and we have no reliable data about luminescence properties of nanocrystalline $CaWO_4$.

2. Experiment

2.1. *Samples.* The cerium doped YAG nanocrystals (powders) with a grain size ~20 nm were obtained by the co-precipitation method. The peculiarities of the synthesis procedure are described in details in [12]. The structure of the nanopowders was controlled by X-ray diffraction analysis. Three samples each having a different cerium concentration (0.5%, 1.5% and 5%) were obtained and studied. The nanopowders obtained were used as raw starting materials for the synthesis of a nanostructured translucent ceramic. The nanoceramic samples were fabricated by means of a high pressure (up to 8 GPa) and low temperature (up to 450^{o}C) technique (see details in [9]). The XRD analysis and SEM images were performed in order to compare the lattice structure and grain size of the starting nanopowders to the sintered nanoceramic samples. It was detected that fabrication process did not cause change in the structure and there was no significant grain growth [9-10]. Luminescence characteristics of the YAG:Ce (5%) single crystal (grown by Czohralski method) have been measured for comparison.

Nanocrystalline $CaWO_4$ (nanopowder) has been synthesized by the simple sol-gel method using tungsten (VI) oxide and calcium nitrate tetrahydrate as starting materials. The detailed description of the synthesis rout is given in [13]. The XRD analysis, SEM images and IR spectroscopy were applied for characterization of obtained $CaWO_4$ nanopowders [13]. Parameters of the sol-gel process have strong influence on the grain size and morphology of the final product. In this paper we present results for three different $CaWO_4$ nanopowders denoted as AK0008, N221 and N222, which have similar average particle size (about 100 nm) but they were synthesized under slightly different conditions. However, there were no any significant differences in the XRD, SEM and IR spectroscopy data for these three samples. Commercial $CaWO_4$ powder (99.78, Alfa Aesar) and the single crystal (Czohralski grown) as a reference material were measured too.

2.2. *Luminescence measurements*. Two types of excitation sources were applied for luminescence measurements: electron beam pulse accelerator and pulsed VUV synchrotron radiation. The pulsed electron beam (e-beam) applied for time-resolved measurements had the following parameters. The electron acceleration voltage 280 keV, pulse duration was 8 ns, and density of excitation was 10^{12} el/cm^2. Luminescence signals were measured via grating monochromator, detected by photomultiplier tube and recorded by storage oscilloscope TDS5052 (Tektronix). Time resolution of the set-up was 7 ns. Photoluminescence measurements were carried out using pulsed synchrotron radiation at the SUPERLUMI station [14] at HASYLAB (DESY, Hamburg).

3. Results and discussion

3.1. *YAG:Ce*. Cerium related emission in YAG:Ce single crystal arises due to transition from 5d excited state to 4f ground state of Ce^{3+} ion [15]. Ground state of Ce^{3+} ion consists on two levels: $^2F_{7/2}$ and $^2F_{5/2}$, and therefore the emission band is split at low temperature. On the Figure 1 is shown the spectra of cerium related emission in Ce^{3+} doped YAG single crystal and 5% cerium doped nanopowders under band-to-band excitation (84 nm or 14.76 eV) at 10 K. As a result of the spectra

decompositions on two separate gauss bands at ~2.38 eV (band A) and ~2.13 eV (band B) have been retrieved in each case (on the picture the decomposition is shown only for the crystal).

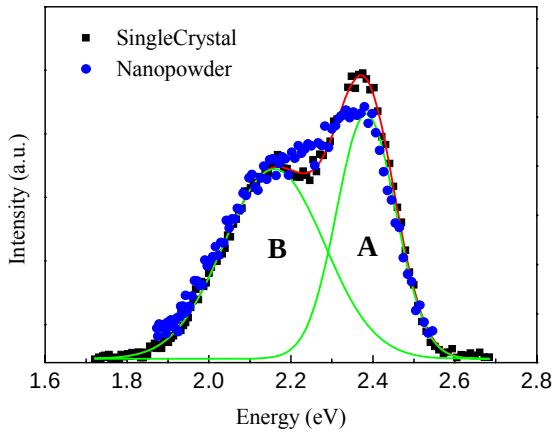

Figure 1. Luminescence spectra of Ce^{3+} emission in YAG single crystal and nanopowder under VUV excitation (14.76 eV) at 10 K. Decomposition on the Gauss is given for the single crystal.

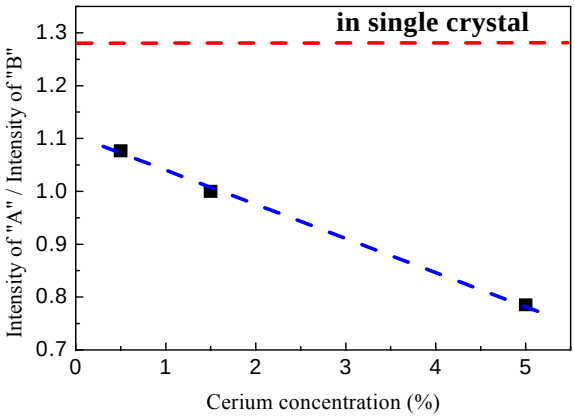

Figure 2. Concentration dependence of the ratio of intensities of the A and B emission bands (squares) which were excited by VUV excitation (14.76 eV) at 10 K. The value for the single crystal is given for the comparison by red dash line.

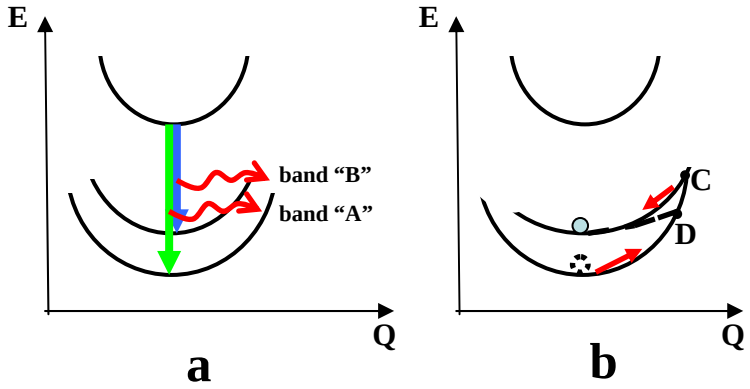

Figure 3. Configurational coordinate model of Ce^{3+} in YAG single crystal (a) and nanocrystals (b).

Spectral positions and band widths of these bands are very close for single and nanocrystals. However, a ratio of intensities of the bands A and B is different for crystal and nanopowder and, moreover, it depends strongly on the Ce^{3+} ions concentration (Figure 2). Interpretation of these results

is based on the suggestion that a local environment around the luminescence centre is different for single crystal and nanopowders. Due to some reasons (surface influence, impurity ions segregation and so on) a local crystalline field (electron-phonon interaction) is slightly distorted in nanocrystals. It leads to perturbation of the one of the adiabatic potential of ground state of Ce^{3+} ion and, as a result, potential curves of two ground states are intersected (point C on the Figure 3). Therefore a hole from lowest ground state can be thermally transferred to the next ground level and correspondingly the contribution of the radiative transition between excited state and lowest ground state decreases. If cerium concentration increases the perturbation of the luminescence centres increases too and cross point of potential curves shifts down (point D on Figure 3) thereby the thermal barrier for holes between two ground states decreases.

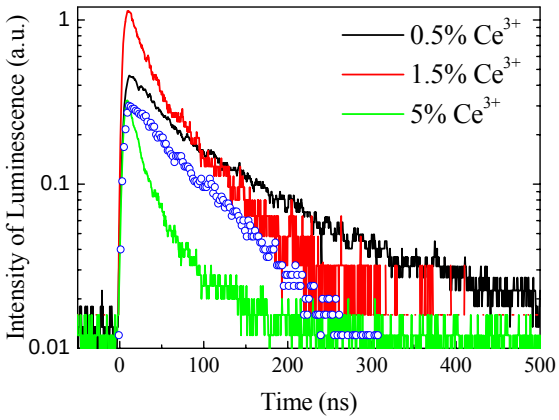

Figure 4. Semi-logarithmic plot of decay kinetics of cerium related emission under e-beam excitation in YAG nanopowders at different Ce^{3+} ions concentration at room temperature. The decay kinetic for the single crystal is given for comparison (open blue circles).

Time-resolved luminescence characteristics of cerium related luminescence have been studied under band-to-band excitation using e-beam accelerator and VUV photons from synchrotron radiation. Decay kinetics of Ce^{3+} emission were the same and, in our measurements, did not depend on the excitation density and excitation mechanism of the luminescence centre. Decay kinetics of Ce^{3+} luminescence of YAG:Ce nanopowders under e-beam excitation at room temperature are depicted on the Figure 4. Corresponding decay kinetic for cerium doped YAG single crystal is also shown for comparison. The decay kinetic for the single crystal obeys the exponential law and characteristic relaxation time in that case is 70-80 ns and this value is in an excellent agreement with the literature data [16]. The decay kinetics and intensities of Ce^{3+} emission in YAG nanopowders are strongly dependant on the concentration of cerium ions. Such important parameters as emission decay time constants (τ) and luminescence light yield are very sensitive to the Ce^{3+} ions contents in nanopowders. In fact, the highest light yield was observed for the sample with 1.5% of Ce^{3+} and significant concentration quenching was observed at 5% of Ce^{3+} in YAG:Ce nanopowders (see details in our previous paper [17]) In the case of nanopowders each of the decay kinetic is not a straight line in semi logarithmic scales and therefore could not be fitted by a single exponent. On the other hand each of them can be approximated by the sum of two exponents with different time constants: fast (τ_1) and slow (τ_2):

$$I = I_1 \exp\left(-\frac{\tau_1}{t}\right) + I_2 \exp\left(-\frac{\tau_2}{t}\right) \quad (1)$$

where I_1 and I_2 are initial intensities of fast and slow processes correspondingly. Parameters of the luminescence relaxation such as τ_1, τ_2 and I_1/I_2 ratio are summarized in the Table 1. Here it is necessary to make short important remark. The deviation from single exponential decay of Ce^{3+} related emission was observed before in YAG single crystal due to the presence of shallow traps [18, 19]. Charge carriers re-trapping on shallow traps leads to longer emission's decay i.e. decay components with time constants longer than the main decay time constant (~80 ns) have been detected

[18]. However, in the case of the nanomaterials the additional decay component (τ_1) is faster than the main one (τ_2) and it can not be caused by influences of shallow traps in nanopowders.

The ratio of the initial intensities of fast and slow components (I_1/I_2) shows the contribution of each component into entire relaxation process. If the cerium concentration in nanopowders increases both components of the decay kinetics become faster. Simultaneously the contribution of the fast component is dominated in heavily doped nanopowders.

Table 1. Parameters of Ce^{3+} related luminescence decay kinetics under e-beam excitation in YAG nanopowders with a different cerium concentration.

Ce^{3+} concentration	0.5%	1.5%	5%
Fast component (τ_1)	33±3 ns	20±3 ns	14±3 ns
Slow component (τ_2)	134±5 ns	90±5 ns	60±5 ns
I_1/I_2	~0.8	~2	~3

It is supposed that there are two different regions in the nanoparticle: "volume" and "surface". If Ce^{3+} ion is located in the "volume" region (Ce^{3+}_V) its position in the lattice and its local surrounding are similar to the position and the local surrounding of the impurity ion in the YAG single crystal. Such Ce^{3+}_V ions have a decay time constant (see data for 1.5% doped sample – the "brightest" nanopowders) close to the decay time of Ce^{3+} in the single crystal, i.e. it is supposed that Ce^{3+}_V ions are responsible for the slow components of the decay kinetics. However, cerium ions in the surface region (Ce^{3+}_S) are strongly perturbed by the surface states and their local symmetry of Ce^{3+}_S is low. Therefore the decay kinetic of Ce^{3+}_S is shorter than of Ce^{3+}_V and the two-exponential decay kinetic of cerium related emission observed in YAG:Ce nanopowders arises from cerium ions being in two different regions of the nanoparticle. At low cerium concentration Ce^{3+} ions are uniformly distributed over the nanoparticle and the contribution of the fast and the slow components of the decay of the cerium related emission is approximately equal. If the cerium concentration increases Ce^{3+} ions tend to occupy positions in surface area that leads to the domination of the fast component. If cerium concentration is high (higher than ~2%) the Ce^{3+} ions segregation occurs near the surface that leads to the concentration quenching of the cerium related luminescence. Indeed, how one can see from Figure 5 the luminescence light yield (the area under decay curve) of the heavily doped samples is obviously significantly lower than for the samples with the low cerium concentration.

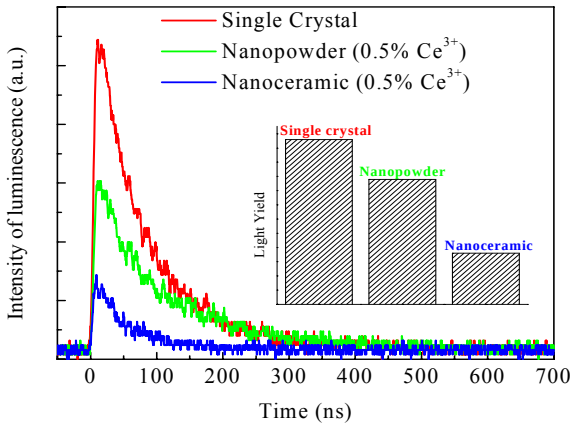

Figure 5. Decay kinetic of cerium related emission in YAG single crystal, nanopowder and nanoceramic under e-beam excitation at room temperature. Luminescence light yield for each sample is shown inset.

The question is naturally arises why cerium ions from different areas of a YAG nanoparticle have different decay times of luminescence? In fact, a transition from 5d excited state to 4f ground state is both parity-allowed and spin-allowed [20] and therefore a slight perturbation of the local symmetry of the luminescence centre could not exert a significant influence upon relaxation time. One of the possible explanations can be that decay time can depend strongly on the energy transfer from host

lattice to Ce^{3+} ions. For instance energy transfer rate to Ce^{3+}_S is higher than to Ce^{3+}_V ions. In fact it is known that in cerium doped YAG single crystal at room temperature a resonance energy transfer from self-trapped excitons to Ce^{3+} ions takes place [21]. It can be speculated that excitons in nanomaterials tend to diffuse to surfaces of nanoparticles. Hence energy transfer from excitons to surface cerium ions is more efficient than to "volume" ions. However such explanation is not correct because two components (fast and slow) in cerium related emission decay were also observed under direct excitation of Ce^{3+} ions in YAG nanopowders [11]. Therefore we suggest another simple model. It is known that the probability of transitions from excited state into ground one depends strongly on the wave functions overlapping [22]. If adiabatic potentials of the luminescence center (Ce^{3+}) in nanomaterials are strongly perturbed the wave functions overlapping can be drastically changed. We suggest that the perturbation of Ce^{3+}_S center leads to the stronger overlapping of wave functions of the excited and ground states. Hence in this case probability of the radiative transition increases and decay time becomes shorter.

The production of the transparent ceramic from YAG nanopowders has high importance from practical application point of view. However sintering processes may change luminescence properties of the material. In fact, decay kinetics of cerium related emission under e-beam excitation obtained for the single crystal, nanopowder (0.5% Ce^{3+}) and nanoceramic (0.5% Ce^{3+}) (Figure 5) are different. Special experiment conditions were provided for in order to compare light yield of luminescence for these three samples. Luminescence light yield in each case was determined as area under the corresponding decay curve and results were summarized on Figure 5 inset. Noteworthy that cerium emission light yield is surprisingly low for the ceramic sample even comparing to raw starting nanopowder. Cerium related emission decay time constants τ_1 and τ_2 are very close for the nanoceramic and nanopowder samples; however the contribution of fast and slow components are different. The ratio of intensities of fast and slow components for the nanoceramic sample is about 5 and this value approximately 5-6 times higher than for the nanopowder (see data from Table 1). Taking into account that grain size of nanoceramic is the same as particle size of the nanopowder peculiar behavior of time-resolved luminescence characteristics in the nanoceramic would be explained in the framework of the model suggested above for the nanopowders. So, significant contribution of the fast component of the Ce^{3+} emission decay kinetic for the nanoceramic shows that the distribution of cerium ions is changed during the sintering process: impurity ions are "forced" from "volume" region to surface region, i.e. Ce^{3+}_V ions diffuse to the surface forming Ce^{3+}_S. As a result Ce^{3+} ions concentration in grain boundaries becomes so high that concentration quenching appears. However, since nanoceramic was sintered at relatively low temperatures the diffusion of Ce^{3+} ions is highly unlikely. Therefore, obviously the change of the decay kinetic for nanoceramic is due to the high pressure applied. Most likely significant damages like dislocations are formed in the nanoceramic under high pressure. Since grain size of nanoceramic is relatively small (~20 nm) big dislocations may act as an "additional" surface and impurity segregation near dislocation lines likewise near grain surface is quite possible.

3.2. *$CaWO_4$.* Luminescence spectra of $CaWO_4$ nanopowders reveal a relatively broad band near 420 nm that coincides with the emission band for the commercial powder and the single crystal. It is known that such intrinsic blue emission in $CaWO_4$ arises due to the spin-forbidden $^3T_1 \rightarrow {}^1A_1$ transition in $(WO_4)^{2-}$ molecular complex [23]. On the other hand excited $(WO_4)^{2-}$ complex can be represented as a self-trapped exciton and blue intrinsic luminescence band is emission of self-trapped exciton [24].

Excitation spectra for this intrinsic luminescence of nanopowders are shown on Figure 6. It clearly seen that the excitation spectra for the samples N221 and N222 are shifted to long-wavelength side or they have an additional absorption band just below the conduction band edge. On the other hand the excitation spectrum for the sample AK0008 even slightly shifted to the short wavelength side relatively to the excitation spectrum of the commercial powder. Moreover it looks that the excitonic band is better resolved in AK0008 nanopowders than in commercial one. So, we can conclude that the

quality of sol-gel synthesized $CaWO_4$ nanopowders is better than of the commercial powder and it is affected on their luminescence properties.

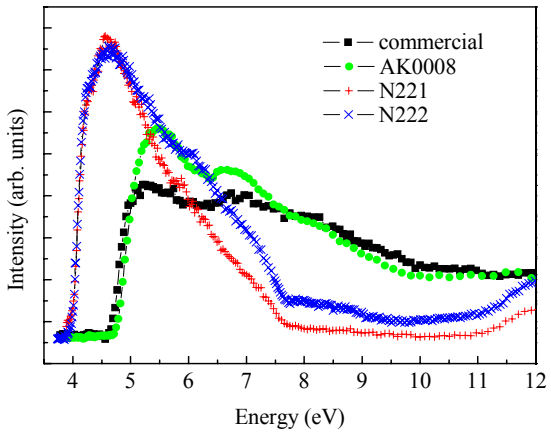

Figure 6. Excitation spectra of blue emission band (420 nm) at 8.5 K for three different $CaWO_4$ nanopowders. The spectrum for the commercial $CaWO_4$ is given for comparison.

These results confirm that luminescence properties of sol-gel synthesized $CaWO_4$ nanopowders depend strongly on the synthesis rout. In our opinion the powders N222 and N221 have a high concentration of some shallow traps therefore spectra for these samples have additional intensive excitation band. If one excites the nanopowders in this defect related band (for example by fourth harmonic of the YAG:Nd laser emitting at 266 nm) the same blue emission band at 2.9 eV is observed, i.e. the same $^3T_1 \rightarrow {}^1A_1$ transition in $(WO_4)^{2-}$ ion occurs. However decay kinetic of this blue emission is significantly faster than the decay kinetic of luminescence single crystal (Figure 7): the main component of the emission in nanopowder is ~35 ns that is at least two order of magnitude faster if compare with luminescence decay time for the single crystal. It is clear because if $(WO_4)^{2-}$ ion is perturbed by nearest shallow trap the spin-forbidden $^3T_1 \rightarrow {}^1A_1$ transition becomes partially-allowed that, in turn, leads to decreasing of luminescence decay time.

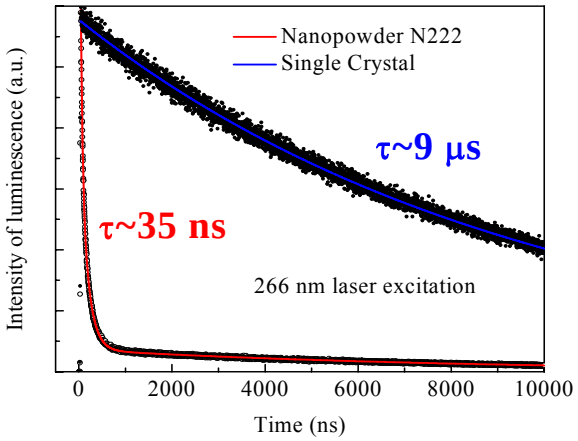

Figure 7. Decay kinetics of blue emission band in $CaWO_4$ single crystal and nanopowders with high concentration of shallow traps under 266 nm laser excitation at room temperature

It is necessary to note that the luminescence decay kinetics of "the best" nanopowder sample (AK0008) are almost the same like for the rather good quality single crystal. It is remarkably, that there were not any components in emission decay kinetics due to surface states in $CaWO_4$ nanopowders which play rather essential role in cerium doped YAG nanopowders. Quite possible that the reason of such discrepancy is that the average grain size of $CaWO_4$ nanopowders was approximately in five times bigger than YAG nanocrystals and surface influence is not so high. Therefore the synthesis and study of CaWO4 nanocrystals with smaller particle size is actual task.

4. Conclusions

Time-resolved luminescence characteristics of prospective nanosized oxides have been studied. It was detected surface states have a significant influence on luminescence properties of cerium doped YAG nanopowders and nanoceramics. For instance it was shown that surface states may cause the perturbation of adiabatic potential of Ce^{3+} ion ground state in YAG nanopowders. Detailed analysis of the time-resolved characteristics of the cerium related emission in YAG nanocrystals allows us to suggest that there are two non-equivalent Ce^{3+} positions in nanoparticles: "volume" and "surface". It was supposed that energy from the host lattice transfers faster to "surface" related Ce^{3+} ions. The model explained the considerable quenching of cerium related luminescence in heavily doped YAG nanopowders as well as YAG nanoceramic has been suggested and discussed. In according of this model the segregation of Ce^{3+} ions near nanoparticles surface and/or dislocation lines plays a crucial role.

Luminescence properties of sol-gel synthesized $CaWO_4$ nanocrystals depend strongly on the quality of the obtained material. The best $CaWO_4$ nanopowders have luminescence properties comparable to the commercial macro powders and the single crystal. Varying the synthesis rout one can govern the time-resolved luminescence characteristics of $CaWO_4$ nanopowders. It opens possibility for wider practical applications of such nanomaterials.

Acknowledgments

This work was supported by LSC grant 05.1720. The work has been granted by DESY and European Community (Contract RII3-CT-2004-506008 (IA-SFS)). V.P. is thankful for European Social Found for the support.

References

[1] C.W.E. Eijk, Radiation Measurements **38 (4-6)** (2004) 337
[2] C.W.E. Eijk, Nucl. Instrum. Meth. Phys. Res. A **509 (1-3)** (2003)17
[3] M. Globus, B. Grinyov, Jong Kyung Kim, Inorganic Scintillators for Modern and Traditional Application (Ukraine, Kharkiv 2005)
[4] M.V. Korzhik, Physics of Single Crystalline Oxide Scintillators (Belarus, Minsk 2003) (in Rissian)
[5] P. Schlotter, R. Schmidt, J. Schneider, Appl. Phys. **A64** (1997) 417
[6] J.A. Mares, M. Nikl, A. Beitlerova, N. Solovieva, C. D′Ambrosio, K. Blazek, P. Maly, K. Nejezchleb, P. Fabeni and G.P. Pazzi, Nucl. Instrum. Meth. Phys. Res. A **537** (2005) 271
[7] V. B. Mikhailik, H. Kraus, D. Wahl M. Itoh, M. Koike and I. K. Bailiff, Phys. Rev. B **69** (2004) 205109
[8] M. Moszynsski, M. Balcerzyk, W. Charnacki, A. Nassalski, T. Szczesniak, H. Kraus, V.B. Mikhailik, I.M. Solskii, Nucl. Instrum. Meth. Phys. Res. A **533** (2005) 578
[9] R. Pązik, P. Głuchowski, D. Hreniak, W. Stręk, M. Roś, R. Fedyk and W. Łojkowski, Optical Materials, article in press, avalible online: doi:10.1016/j.optmat.2007.02.017
[10] T. Chudoba, M. Teyssier and W. Lojkowski, Solid State Phenomena, **128** (2007) 41
[11] V. Pankratov, L. Grigorjeva, D. Millers, T. Chudoba, Radiation Measurements, **42** (2007) 679
[12] H. Wang, L. Gao and K. Niihara, Material Science and Engineering A **288** (2000) 1
[13] A. Katelnikovas, L. Grigorjeva, D. Millers, V. Pankratov and A. Kareiva, Lithuanian Journal of Physics **47** (2007) 63
[14] G. Zimmerer, Nuclear Inst. and Methods in Phys. Res. A **308** (1991) 178
[15] R.R. Jacobs, W.F. Krupke, M.J. Weber, Appl. Phys. Lett. **33** (1978) 410
[16] S. Derenzo, W. Moses, Proceedings of the Inter. Conference on „Crystal 2000" (1992) p.125
[17] V. Pankratov, L. Grigorjeva, D. Millers, T. Chudoba, R. Fedyk and W. Lojkowski, Solid State Phenomena **128** (2007) 173

[18] E. Zych. C. Brecher, J. Glodo, J. Phys.: Condens. Matter **12** (2000) 1947
[19] D.J. Robbins, B. Cockayne, B. Lent, C.N. Duckworth and J.L. Glasper, Phys. Rev. B **19** (1979) 1254
[20] G. Blasse, W.L. Wanmaker, J.W. Tervrugt and A. Bril, Philips Res. Rept. **23** (1968) 189
[21] M.J Weber, S.E Derenzo and W.W Moses, Journal of Luminescence **87-89** (2000) 830
[22] A.M. Stoneham, Theory of defects in Solids, Clarendon Press, Oxford 1975
[23] G. Blasse, Structure and Bonding **42** (1980) 1
[24] M. Itoh, M. Fuita, Phys. Rev. B **62** (2000) 12825